We are IntechOpen,
the world's leading publisher of Open Access books
Built by scientists, for scientists

6,900
Open access books available

186,000
International authors and editors

200M
Downloads

154
Countries delivered to

Our authors are among the

TOP 1%
most cited scientists

12.2%
Contributors from top 500 universities

CLARIVATE ANALYTICS
BOOK CITATION INDEX
INDEXED

WEB OF SCIENCE™

Selection of our books indexed in the Book Citation Index
in Web of Science™ Core Collection (BKCI)

Interested in publishing with us?
Contact book.department@intechopen.com

Numbers displayed above are based on latest data collected.
For more information visit www.intechopen.com

Electrodeposited Cu₂O Thin Films for Fabrication of CuO/Cu₂O Heterojunction

Ruwan Palitha Wijesundera
Department of Physics, University of Kelaniya, Kelaniya
Sri Lanka

1. Introduction

Solar energy is considered as the most promising alternative energy source to replace environmentally distractive fossil fuel. However, it is a challenging task to develop solar energy converting devices using low cost techniques and environmentally friendly materials. Environmentally friendly cuprous oxide (Cu_2O) is being studied as a possible candidate for photovoltaic applications because of highly acceptable electrical and optical properties. Cu_2O has a direct band gap of 2 eV (Rakhshani, 1986; Siripala et al., 1996), which lies in the acceptable range of window material for photovoltaic applications. It is a stoichiometry defect type semiconductor having a cubic crystal structure with lattice constant of 4.27 Å (Ghijsen et al., 1988; Wijesundera et al., 2006). The theoretical conversion efficiency limit for Cu_2O based solar cells is about 20% [5].

Thermal oxidation was a most widely used method for the preparation of Cu_2O in the early stage. It gives a low resistive, p-type polycrystalline material with large grains for photovoltaic applications. It was found that Cu_2O grown at high temperature has high leakage-current due to the shorting paths created during the formation of the material, and it causes low conversion efficiencies. Therefore it was focused to prepare Cu_2O at low temperature, which may provide better characteristics in this regard. Among the various Cu_2O deposition techniques (Olsen et al., 1981; Aveline & Bonilla, 1981; Fortin & Masson, 1981; Roos et al., 1983; Sears & Fortin, 1984; Rakhshani, 1986; Rai, 1988; Santra et al., 1992; Musa et al., 1998; Maruyama, 1998; Ivill et al., 2003; Hames & San, 2004; Ogwa et al., 2005), electrodeposition (Siripala & Jayakody, 1986, Siripala et al., 1996; Rakhshani & Varghese, 1987a, 1988b; Mahalingam et al., 2004; Tang et al., 2005; Wijesundera et al., 2006) is an attractive one because of its simplicity, low cost and low-temperature process and on the other hand the composition of the material can be easily adjusted leading to changes in physical properties. Most of the techniques produce p-type conducting thin films. Many theoretical and experimental studies (Guy, 1972; Pollack & Trivich, 1975; Kaufman & Hawkins, 1984; Harukawa et al., 2000; Wright & Nelson, 2002; Paul et al., 2006) have been revealed that the Cu vacancies originate the p-type conductivity. However, electrodeposition (Siripala & Jayakody, 1986, Siripala et al., 1996; Wijesundera et al., 2000; Wijesundera et al., 2006) of Cu_2O thin films in a slightly acidic aqueous baths produce n-type conductivity. Further it has been reported that the origin of this n-type behavior is due to oxygen vacancies and/or additional copper atoms. Recently, Garutara *et al.* (2006) carried out the photoluminescence (PL) characterisation for the electrodeposited n-type

polycrystalline Cu_2O, and confirmed that the n-type conductivity is due to the oxygen vacancies created in the lattice. This n-type conductivity of Cu_2O is very important in developing low cost thin film solar cells because the electron affinity of Cu_2O is comparatively high. This will enable to explore the possibility of making heterojunction with suitable low band gap p-type semiconductors for application in low cost solar cells.

Most of the properties of the electrodeposited Cu_2O were reported to be similar to those of the thermally grown film (Rai, 1988). The electrodeposition of Cu_2O is carried out potentiostatically or galvanostatically (Rakhshani & Varghese, 1987a, 1988b; Mahalingam et al., 2000; Mahalingam et al., 2002). Dependency of parameters (concentrations, pH, temperature of the bath, deposition potential with deposits) had been investigated by several research groups (Zhou & Switzer, 1998; Mahalingam et al., 2002; Tang et al., 2005; Wijesundera et al., 2006). The results showed that electrodeposition is very good tool to manipulate the deposits (structure, properties, grain shape and size, etc) by changing the parameters. Various electrolytes such as cupric sulphate + ethylene glycol alkaline solution, cupric sulphate aqueous solution, cupric sulphate + lactic acid alkaline aqueous solution, cupric nitrate aqueous solution and sodium acetate+ cupric acetate aqueous solution, have been reported in the electrodeposition of Cu_2O.

Cu_2O-based heterojunctions of ZnO/Cu_2O (Herion et al., 1980; Akimoto et al., 2006), CdO/Cu_2O (Papadimitriou et al., 1981; Hames & San, 2004), ITO/Cu_2O (Sears et al., 1983), TCO/Cu_2O (Tanaka et al., 2004), and Cu_2O/Cu_xS (Wijesundera et al., 2000) were studied in the literature, and the reported best values of V_{oc} and J_{sc} were 300 mV and 2.0 mA cm^{-2}, 400 mV and 2.0 mA cm^{-2}, 270 mV and 2.18 mA cm^{-2}, 400 mV and 7.1 mA cm^{-2}, and 240 mV and 1.6 mA cm^{-2}, respectively.

Cupric oxide (CuO) is one of promising materials as an absorber layer for Cu_2O based solar cells because it is a direct band gap of about 1.2 eV (Rakhshani, 1986) which is well matched as an absorber for photovoltaic applications. It is also stoichiometry defect type semiconductor having a monoclinic crystal structure with lattice constants a of 4.6837 Å, b of 3.4226 Å, c of 5.1288 Å and β of 99.54° (Ghijsen et al., 1988). CuO had been wildly used for the photocatalysis applications. However, CuO as photovoltaic applications are very limited in the literature. The photoactive CuO based dye-sensitised photovoltaic device was recently reported by the Anandan *et al*. (2005) and we reported the possibility of fabricating the p-CuO/n-Cu_2O heterojunction (Wijesundera, 2010).

2. Growth and characterisation of electrodeposited Cu_2O

Electrodeposition is a simple technique to deposit Cu_2O on the large area conducting substrate in a very low cost. Electrodeposition of Cu_2O from an alkaline bath was first developed by Starek in 1937 (Stareck, 1937) and electrical and optical properties of electrodeposited Cu_2O were studied by Economon (Rakhshani, 1986). Rakshani and co-workers studied the electrodeposition process under the galvanostatic and potentiostatic conditions using aqueous alkaline $CuSO_4$ solution, to investigate the deposition parameters and properties of the material. Properties of the electrodeposited Cu_2O were reported to be similar to those of the thermally grown films (Rai, 1988) except high resistivity. Siripala *et al*. (Siripala & Jayakody, 1986) reported, for the first time, the observation of n-type photoconductivity in the Cu_2O film electrodes prepared by the electrodeposition on various metal substrates in slightly basic aqueous $CuSO_4$ solution in 1986. However, we have reported that electrodeposited Cu_2O thin films in a slightly acidic acetate bath attributed n-type conductivity.

Potentiostatic electrodeposition of Cu$_2$O thin films on Ti substrates can be investigated using a three electrode electrochemical cell containing an aqueous solution of sodium acetate and cupric acetate. Cupric acetate are used as Cu^{2+} source while sodium acetate are added to the solution making complexes releasing copper ions slowly into the medium allowing a uniform growth of Cu$_2$O thin films. The counter electrode is a platinum plate and reference electrode is saturated calomel electrode (SCE). Growth parameters (ionic concentrations, temperature, pH of the bath, and deposition potential domain) involved in the potentiostatic electrodeposition of the Cu$_2$O thin films can be determined by the method of voltommograms.

voltammetric curves were obtained in a solution containing 0.1 M sodium acetate with the various cupric acetate concentrations, while temperature, pH and stirring speed of the baths were maintained at values of 55 °C, 6.6 (normal pH of the bath) and 300 rev./min respectively. Curve a) in Fig. 1 is without cupric acetate and curves b), c) and d) are cupric acetate concentrations of 0.25 mM, 1 mM and 10 mM respectively. Significant current increase can not be observed in absence with cupric acetate and cathodic peaks begin to form with the introduction of Cu^{2+} ions into the electrolyte. Two well defined cathodic peaks are resulted at –175 mV and –700 mV Vs SCE due to the presence of cupric ions in the electrolyte and these peaks shifted slightly to the anodic side at higher cupric acetate concentrations. First cathodic peak at –175 mV Vs SCE attributes to the formation of Cu$_2$O on the substrate according to the following reaction.

$$2Cu^{2+} + H_2O + 2e^- \Rightarrow Cu_2O + 2H^+$$

Second cathodic peak at –700 mV Vs SCE attributes to the formation of Cu on the substrate according to the following reaction.

$$Cu^{2+} + 2e^- \Rightarrow Cu$$

By examining the working electrode, it can be observed that the electrodeposition of deposits on the substrate is possible in the entire potential range. However, as revealed by the curves in Fig. 1, at higher concentrations the peaks are getting broader and therefore the formation of Cu and Cu$_2$O simultaneously is possible at intermediate potentials (curve d of Fig. 1). The deposition current slightly increases and the peaks are slightly shifted to the positive potential side as increasing the bath temperature range of 25 ˚C to 65 ˚C.

Fig. 2 shows the dependence of the voltammetric curves on the pH of the deposition bath. It is seen that cathodic peak corresponding to the Cu deposition is shifted anodically by about 500 mV and cathodic peak corresponding to the Cu$_2$O deposition is shifted anodically by about 100 mV. This clearly indicates that acidic bath condition favours the deposition of copper over the Cu$_2$O deposition and the possibility of simultaneous deposition of Cu and Cu$_2$O even at lower cathodic potentials. This is further investigated in the following sections.

The potential domain of the first cathodic peak gives the possible potentials for the electrodeposition of Cu$_2$O films while second cathodic peak evidence the possible potential domain for the electrodeposition of Cu films. It is evidence that Cu$_2$O can be electrodeposited in the range of 0 to -300 mV Vs SCE and Cu can be electrodeposited in the range of -700 to -900 mV Vs SCE. The potential domains of the electrodepostion of Cu$_2$O and Cu are independent of the Cu^{2+} ion concentration and the temperature of the bath. However, the deposition rate is increased with the increase in the concentration or the temperature of the bath.
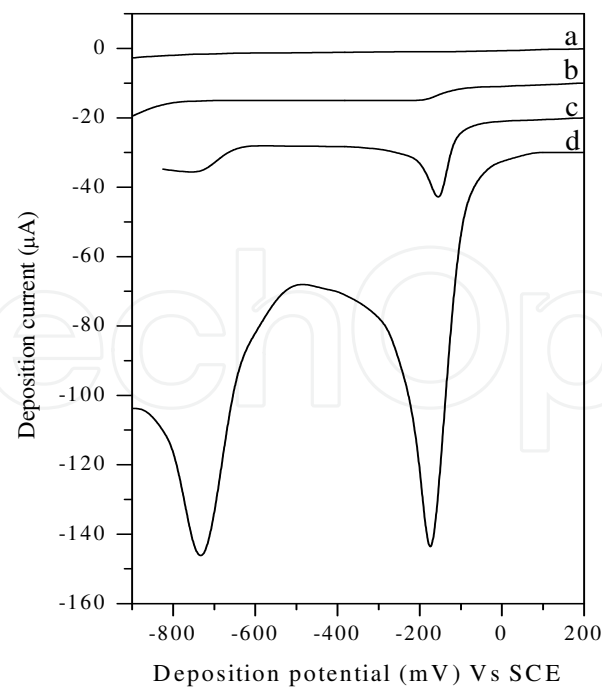
Fig. 1. Voltammetric curves of the Ti electrode (4 mm²) obtained in a solution containing
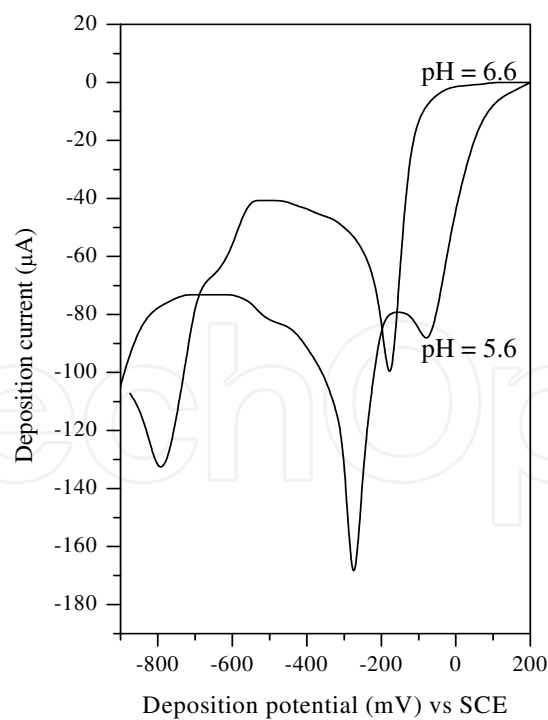0.1 M sodium acetate and cupric acetate concentrations of a) 0 mM, b) 0.25 mM, c) 1 mM and
d) 10 mM

Fig. 2. Voltammetric curves of the Ti electrode (4 mm²) in an electrochemical cell containing
0.1 M sodium acetate and 0.01 M cupric acetate solutions at two different pH values
(pH was adjusted by adding diluted HCI).

Cu$_2$O film deposition potential domain can be further verified by the X-ray diffraction (XRD) spectra obtained for the films electrodeposited at various potentials (-100 to -900 mV Vs SCE). Fig. 3 shows the XRD spectra of the films deposited at a) -200 mV Vs SCE, b) -600 mV Vs SCE and c) -800 mV Vs SCE on Ti substrates in a bath containing 0.1 M sodium acetate and 0.01 M cupric acetate aqueous solution. Fig. 3(a) shows five peaks at 2θ values of 29.58°, 36.43°, 42.32°, 61.39° and 73.54° corresponding to the reflections from (110), (111), (200), (220) and (311) atomic plans of Cu$_2$O in addition to the Ti peaks. Fig. 3(b) exhibits three additional peaks at 2θ values of 43.40°, 50.55° and 74.28° corresponding to the reflection from (111), (200) and (220) atomic plans of Cu in addition to the peaks corresponding to the Cu$_2$O and Ti substrate. It is evident that the intensity of Cu peaks increases with increase of the deposition potential with respect to the SCE while decreasing the intensities of Cu$_2$O peaks. Peaks corresponding to the Cu$_2$O disappeared with further increase in deposition potential. XRD of Fig. 3(d) exhibits peaks corresponding to Cu and Ti only. Thus, in the acetate bath single phase polycrystalline Cu$_2$O thin films with a cubic structure having lattice constant 4.27 Å are possible only with narrow potential domain of 0 to -300 mV Vs SCE while Cu thin films having lattice constant 3.61 Å are possible at potential –700 mV and above Vs SCE.
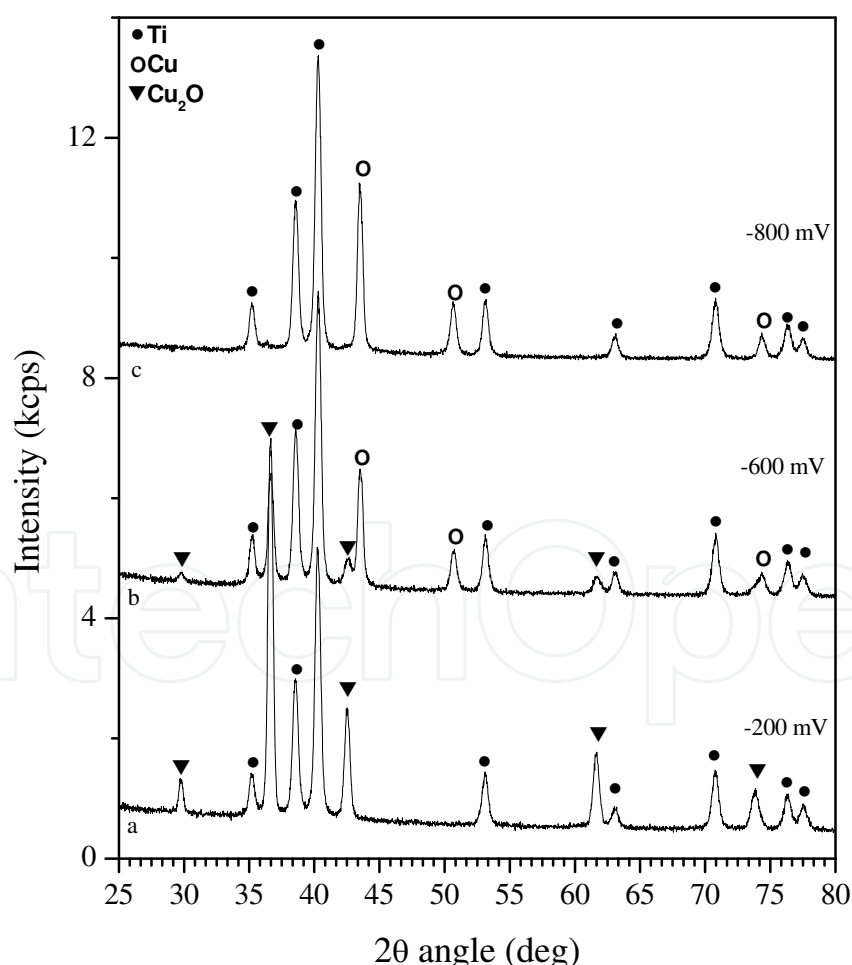

Fig. 3. XRD spectra obtained for the films deposited on Ti substrate at the potentials (a) -200 mV Vs SCE, (b) -600 mV Vs SCE and (c) -800 mV Vs SCE

Fig. 4 shows the scanning electron micrographs (SEMs) of the above set of samples. It is evident that the surface morphology depends on the deposition potential and the films grown on Ti substrate are uniform and polycrystalline. Grain size of Cu_2O is in the range of ~1-2 μm. It is observed that the Cu_2O thin film deposited at –200 mV Vs SCE exhibit cubic structure (Fig. 4(a)) and deviation from the cubic structure can be observed when deposition potential deviate from the -200 mV Vs SCE. Thus, polycrystalline Cu_2O thin films with cubic grains are possible only within a very narrow potential domain of around –200 mV Vs SCE. Fig. 4(b) shows the existence of spherical shaped Cu on top of Cu_2O when film deposited at –400 mV Vs SCE. The co-deposition of Cu with Cu_2O is evident in the XRD spectra, too. This small grains of Cu distributed over the Cu_2O surface will be useful in some other applications. It is clear from XRD and SEM results that Cu_2O, Cu_2O + Cu, and Cu microcrystalline thin films can be separately electrodeposited on Ti substrate by changing the deposition potential from –100 mV to –900 mV Vs SCE using the same electrolyte.

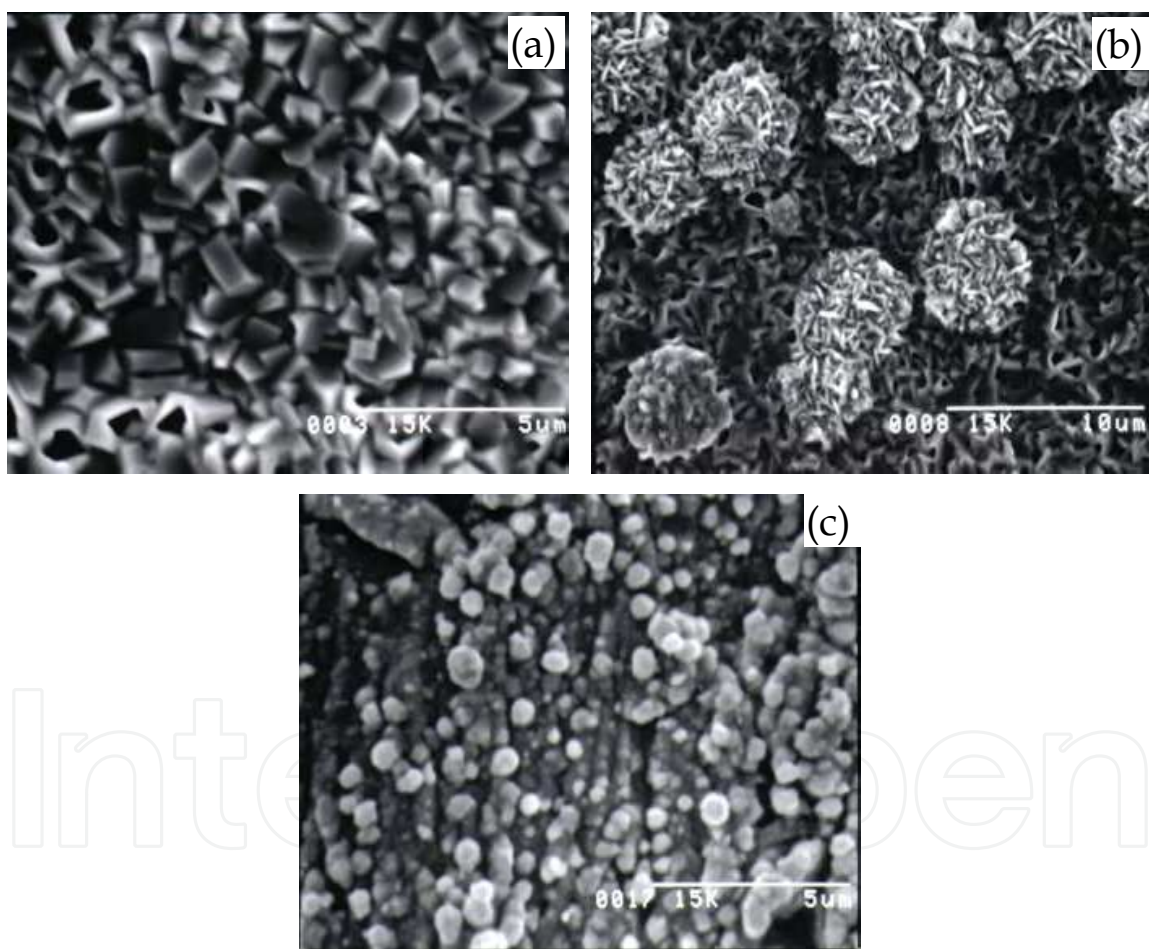Fig. 4. Scanning electron micrographs of thin films electrodeposited at (a) -200 mV Vs SCE, (b) -400 mV Vs SCE and (c) -800 mV Vs SCE

Cu_2O thin films produce negative photovoltages in a photelectrochemical cell (PEC) containing 0.1 M sodium acetate under the white light illumination of 90 W/m². Active area of the film in a PEC was ~1 mm². The magnitudes of the photovoltage and the photocurrent of Cu_2O films deposited at –100 mV to –500 mV Vs SCE were 125 mV and 5 μA, 168 mV and 6.5 μA, 172 mV and 8 μA, 210 mV and 15 μA and 68 mV and 1 μA respectively. Also Cu_2O

film deposited at –600 mV Vs SCE shows the photoactivity but magnitudes of the photovoltage and photocurrent were very small. The best photoresponse we have obtained for the Cu_2O thin film deposited at –400 mV Vs SCE. This may be due to the better charge transfer process between Cu_2O and electrolyte due to the randomly distributed Cu spheres on top of Cu_2O thin films as shown in Fig. 4.

The optical absorption measurements of the Cu_2O thin films on indium doped tin oxide (ITO) substrate deposited at -100 mV to -600 mV Vs SCE indicate that the electrodeposited Cu_2O has a direct band gap of 2.0 eV, and the band gap of the material is independent of the deposition potential.

Photoactivity of the films was further studied by the dark and light current-voltage measurements. Fig. 5 shows the dark and light current-voltage characteristics in a PEC of the films deposited at (a) –200 mV and (b) –400 mV Vs SCE. Current-voltage measurements were obtained in three electrode electrochemical cell. The change of the sign of the photocurrent with the applied voltage shows the evidence for the existence of two junctions within the Ti/Cu_2O/electrolyte system. Particularly with the positive applied bias voltage, the Cu_2O/electrolyte junction become dominant and thereby the n-type photosignal is produced, when negative bias voltage is applied the Ti/Cu_2O junction become dominant and therefore a p-type signal is produced. Similar results have been reported earlier on the ITO/Cu_2O/electrolyte system (Siripala et al., 1996) and $ITO/Cu_2O/Cu_xS$ system (Wijesundera et al., 2000). It has been reported earlier that both n- and p-type photosignals can be obtained in the currant–voltage scans due to the existence of Ti/Cu_2O and Cu_2O/electrolyte Schottky type junctions. The enhancement of n-type signal could be due to the enhancement of Cu_2O/electrolyte junction as compared with the Ti/Cu_2O junction.
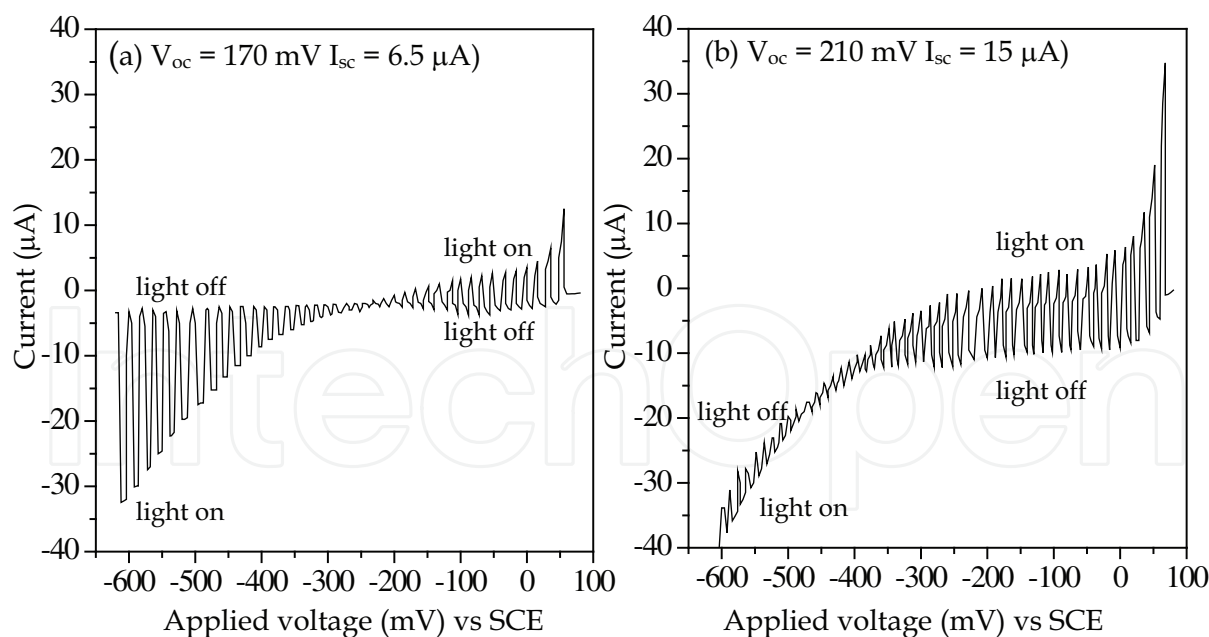

Fig. 5. Dark and light current-voltage characteristics for the films deposited at (a) -200 mV and (b) -400 mV Vs SCE in a PEC containing 0.1 M sodium acetate under the white light illumination of 90 W/m² (effective area of the film is ~1 mm²).

Single phase polycrystalline n-type Cu_2O thin films can be potentiostatically electrodeposited on conducting substrates selecting proper deposition parameters and these

films are uniform and well adhered to substrate. Garutara *et al*. (Garuthara & Siripala, 2006) carried out the photoluminescence (PL) characterisation for the electrodeposited n-type polycrystalline Cu_2O. They showed the existence of the donor energy level of 0.38 eV below the bottom of the conduction band due to the oxygen vacancies and confirmed that the n-type conductivity is due to the oxygen vacancies created in the lattice. Previously reported electrodeposited Cu_2O in a various deposition bath, except slightly acidic acetate bath, attribute p-type conductivity due to the Cu vacancies created in the lattice as thermally grown films.

3. Growth and characterisation of CuO thin films

It is expected that Cu_2O thin films can be oxidized by the annealing in air and thus converted into CuO. Therefore, annealing effects of the electrodeposited Cu_2O thin films in air were investigated in order to obtain a single phase CuO thin films on Ti substrate. Cu_2O thin films on Ti substrates were prepared under the potentiostatic condition of -200 mV Vs SCE for 60 min. in the three electrode electrochemical cell containing 0.1 M sodium acetate and 0.01 M cupric acetate aqueous solution. Temperature of the bath was maintained to 55 ˚C and the electrolyte was continuously stirred using a magnetic stirrer. All the thin films are uniform and having a thickness of about 1 μm which was calculated by monitoring the total charge passed during the film deposition through the working electrode (WE).

The bulk structure of the films, which were annealed at different temparatures and durations, can be determined by XRD measurements and Fig. 6 shows the XRD spectra of the films annealed at 150 to 500 ˚C in air, in addition to the as grown Cu_2O. Results show that Cu_2O structure remains stable even though films are annealed at 300 ˚C, as reported by Siripala *et al*. (1996). Formation of CuO structure can be observed when films are aneealed at
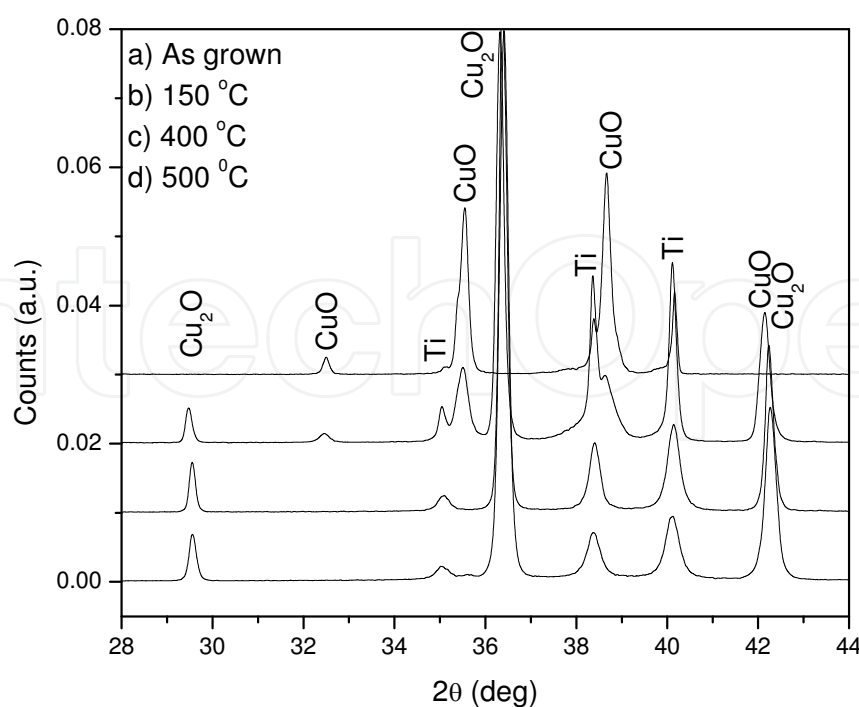

Fig. 6. X-ray diffraction patterns of electrodeposited Cu_2O thin films a) as grown and annealed at b) 150 ºC, c) 400 ºC and d) 500 ºC

400 °C for 15 min. Fig. 6 shows that the intensities of the peaks correspondent to the CuO structure increases while intensities of the peaks correspondent to the Cu₂O structure decreases with the increasing of annealing temperature and duration. The reflections from the Cu₂O structure disappear when the film is annealed at 500 ˚C for 30 min. in air. It is reveled that the single phase CuO thin films on Ti substrate can be prepared by annealing Cu₂O in air.

The surface morphology of the annealing Cu₂O thin films is studied with SEMs. Fig. 7 shows SEMs of (a) as grown, and annealed in air at (b) 175 ˚C, (c) 400 ˚C and (d) 500 ˚C. Results reveal that, by increasing the annealing temperature, the size of the cubic shape polycrystalline grain gradually increase up to 200 ˚C, change to the different shape at 400 °C and converted to the monoclinic like shape polycrystalline grain at 500 °C. Cu₂O thin films have the cubic-like polycrystalline grains. SEMs clearly show that structural phase transition take place from Cu₂O, Cu₂O-CuO, CuO as reveal by the XRD patterns. CuO crystallites are in the order of 250 nm.
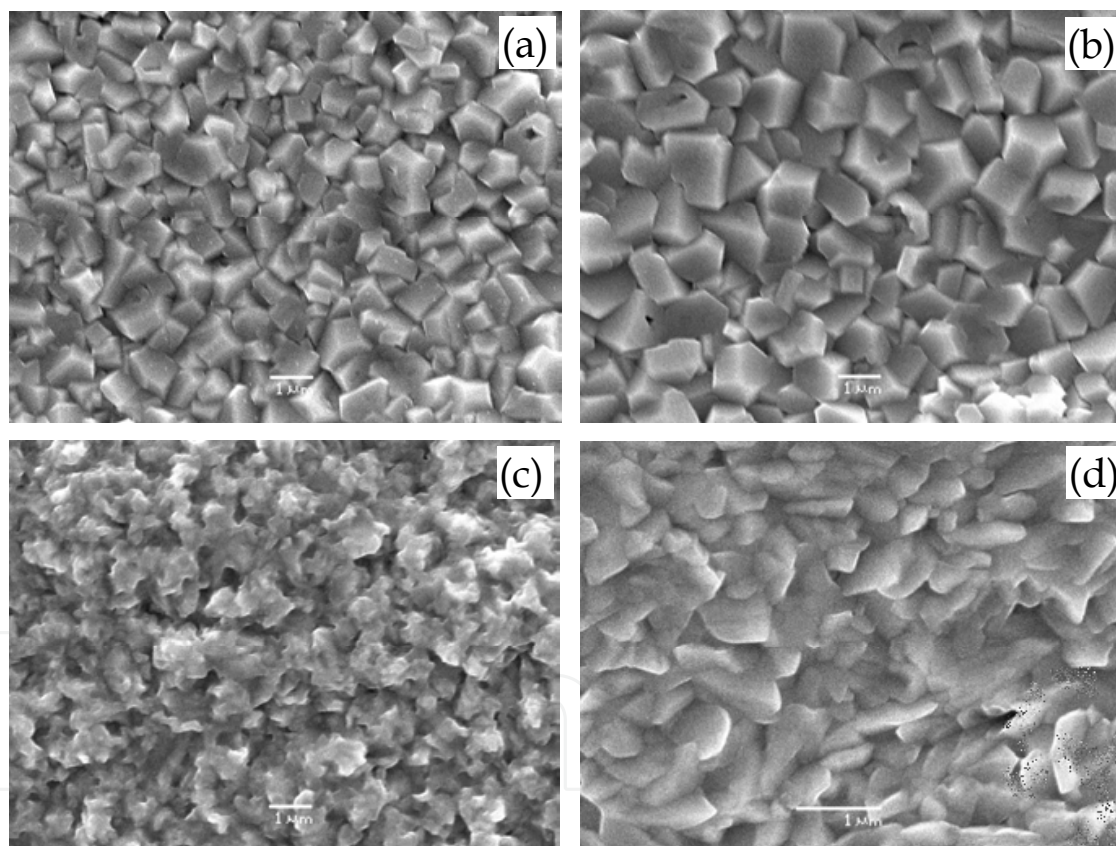

Fig. 7. Scanning electron micrographs of the electrodeposited semiconductor Cu₂O thin films a) as grown and annealed in air at (b) 175 ˚C, (c) 400 ˚C and (d) 500 ˚C

Photosensitivity (V_{oc} and I_{sc}) of the annealed electrodeposited Cu₂O thin films in a two electrode PEC cell containing 0.1 M sodium acetate aqueous solution, under white light illumination of 90 W/m², shows that initial n-type photoconductivity changes to the p-type after annealing 300 °C. Type of the photoconductivity of the Cu₂O thin films can be converted from n- to p-type with annealing because of Cu₂O structure remain same even if films annealed at 300 °C as revealed by XRD patterns.
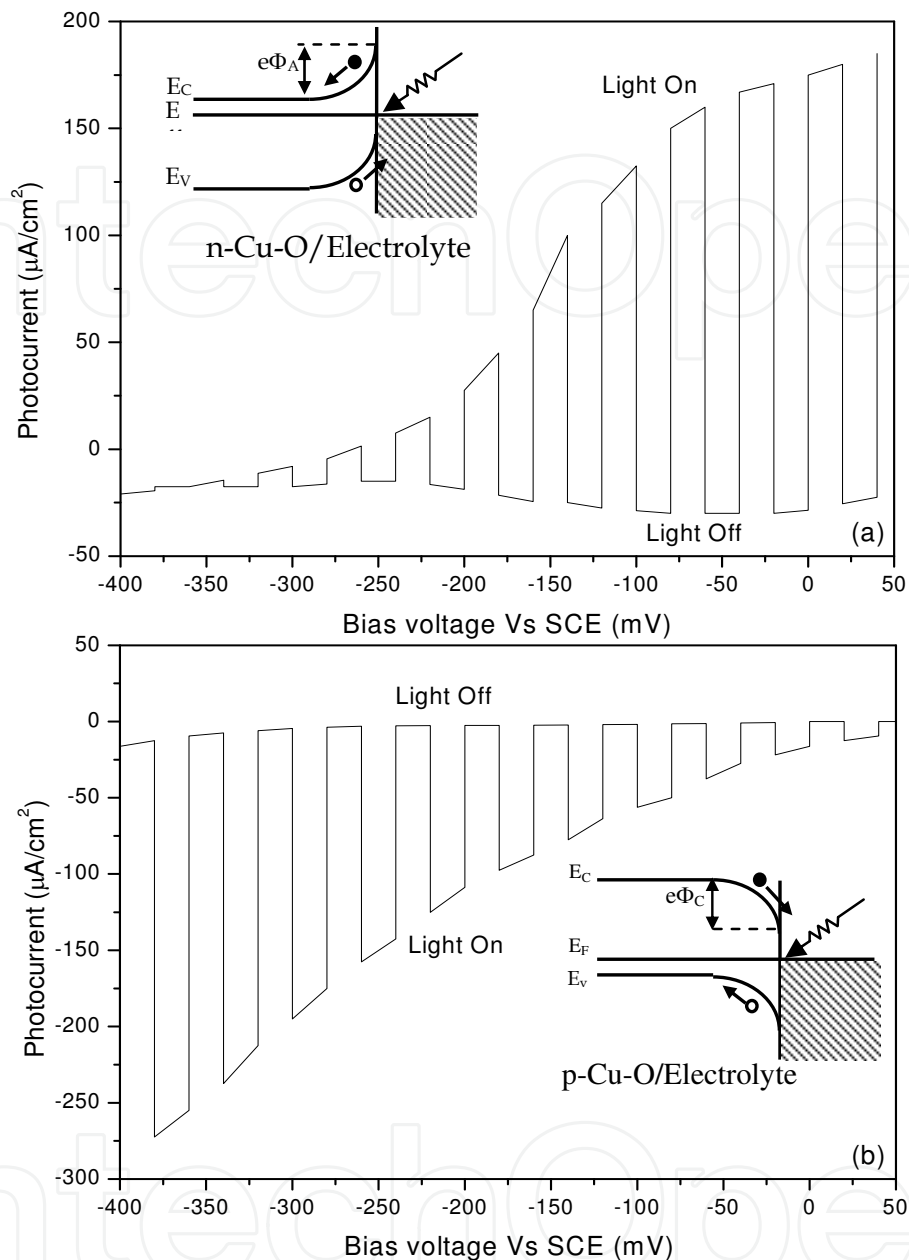
Fig. 8. Dark and light current voltage characteristics of electrodeposited Cu_2O thin film electrodes annealed at (a) 250 ˚C and (b) 300 ˚C. Energy level diagrams for n-type and p-type Cu_2O films in the electrolyte are shown in the insets, where the electron, hole, anodic and cathodic potential are denoted by solid and open circles, $e\Phi_A$ and $e\Phi_C$ respectively.

The photoactivity of the thin films has been further studied by the dark and light current voltage characteristics in a three electrode electrochemical cell. The counter and the reference electrodes are Pt plate and SCE, respectively. The bias voltage has been applied to the working electrode (Ti/Cu_2O) with respect to the SCE. Fig. 8 shows the dark and light

current-voltage characteristics of the thin films annealed at (a) 250 ˚C and (b) 300 ˚C. The similar behaviour is observed for the thin films annealed at less than 250 ˚C and annealed at grater than 300 ˚C, respectively, and is reproducible for each film. In Fig. 8(a), the anodic photocurrent increases with increasing the anodic potential. This suggests that the n-type photoconductivity is due to an anodic potential behaviour, and is reproducibly observed for the thin films annealed at < 250 ˚C. This suggests that the n-type photoconductivity is due to the anodic potential barrier formed at the semiconductor/electrolyte interface, as the inset of Fig. 8(a). However, the photocurrent-potential behaviour is completely changed for the film annealed at ≥ 300 ˚C. In Fig. 8(b), the cathodic photocurrent results from the cathodic potential barrier formed at the interface, as shown in the inset. This cathodic photoresponse assures that the electrical conductivity of the electrodeposited Cu$_2$O films can be changed from the n-type to p-type property by annealing in air. Fig. 9 shows the dark and light current-voltage characteristics of the CuO thin film in a PEC cell containing 0.1 M sodium acetate aqueous solution. The cathodic photocurrent is produced in the range from the anodic to cathodic bias potentials, and the cathodic photocurrent increases with increasing the cathodic potential. This suggests that the p-type photoconductivity is due to the cathodic potential barrier forms at the semiconductor/electrolyte interface. It reveals that the electrodeposited CuO thin films are p-type semiconductors.

Structural phase transition from Cu$_2$O to CuO with annealing and the quality of thin films can be further investigated using Extended X-ray Absorption Fine Structure (EXAFS) which gives local structure around Cu ions. Fig. 10 shows the X-ray absorption spectra (XAS) in the region of 8800 to 9430 eV near the Cu-K edge for the thin films, annealed at 150, 400, and 500 ˚C by using the florescence detection (FD) method. XAS suggest that the local structures around Cu ions in the annealed Cu$_2$O thin films are remain same when films annealed at less than 300 ºC and significantly different when films annealed at grater than 300 ºC.

Refinements of a Fourier transformation spectrum |F(R)| obtained from the oscillating EXAFS spectra can be used to study the quality of Cu$_2$O and CuO thin films. Fig. 11, solid circles show the observed |F(R)| of the thin film annealed at 150 ˚C, where the abscissa is a radial distance (R(Å)) from a X-ray absorbing Cu ion to its surrounding cations and anions. Fig. 11, a solid line shows a theoretical |F(R)|. The refinement produces a good fit between the observed and theoretical |F(R)| indicating the local structure around Cu ions of the film is verymuch similar to the ideal Cu$_2$O structure. Fig. 12 is similar refinement for CuO thin film. These results convince that the thin films are high quality single phase Cu$_2$O and CuO structures (free of amorphous phases and impurities). Detail investigation has been reported (Wijesundera et al., 2007).

It is characterised that single phase Cu$_2$O thin films are converted to two phase Cu$_2$O and CuO composit films with increasing the annealing temperature. Single phase CuO thin films can be obtained by annealing at 500 ºC for 30 min in air. Extended X-ray absorption fine structure (EXAFS) near the Cu K edge of the Cu$_2$O thin films (annealed at 150 ºC for 15 min.) and CuO thin films (annealed at 500 ºC for 30 min.) are confirmed that the films are high quality single phase Cu$_2$O and CuO (free of amophous phases) respectively. Conductivity type of the films strongly depends on the annealing treatment. n-type conductivity of the Cu$_2$O thin films are changed to p-type when the films are annealed at 300 ºC. CuO thin films are photoactive and p-type in a PEC containing 0.1 M sodium acetate.
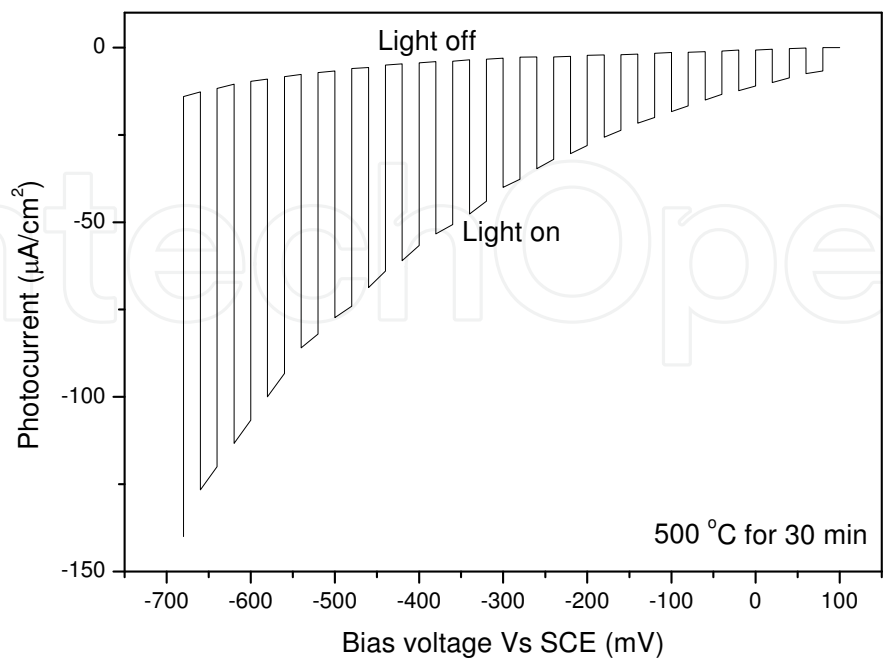
Fig. 9. Dark and light current voltage characterisation of CuO thin film in a PEC cell containing 0.1 M sodium acetate aqueous solution.
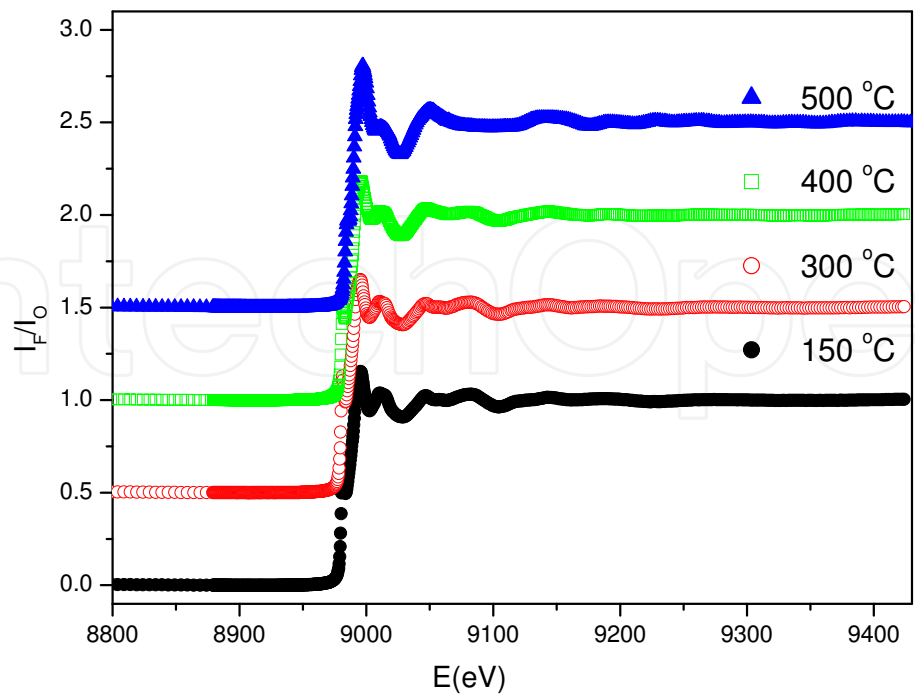

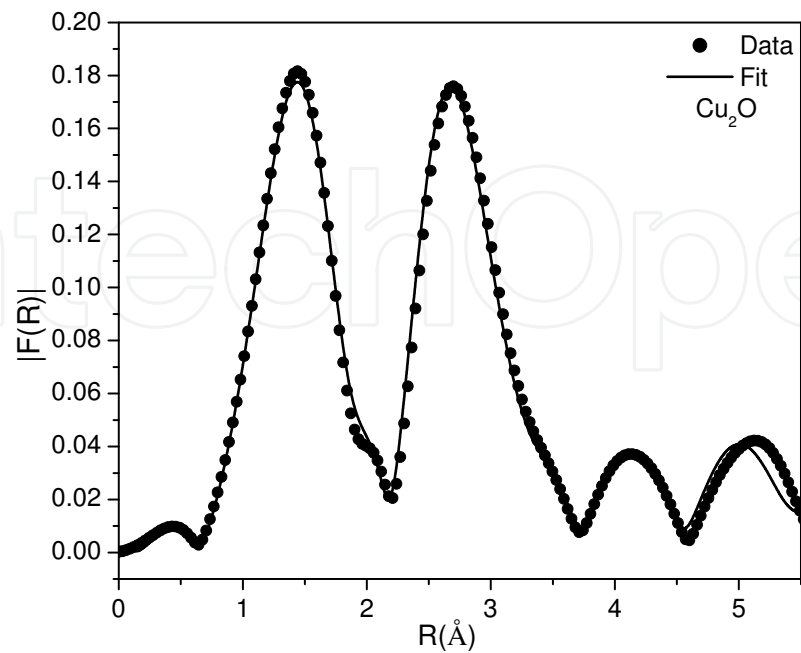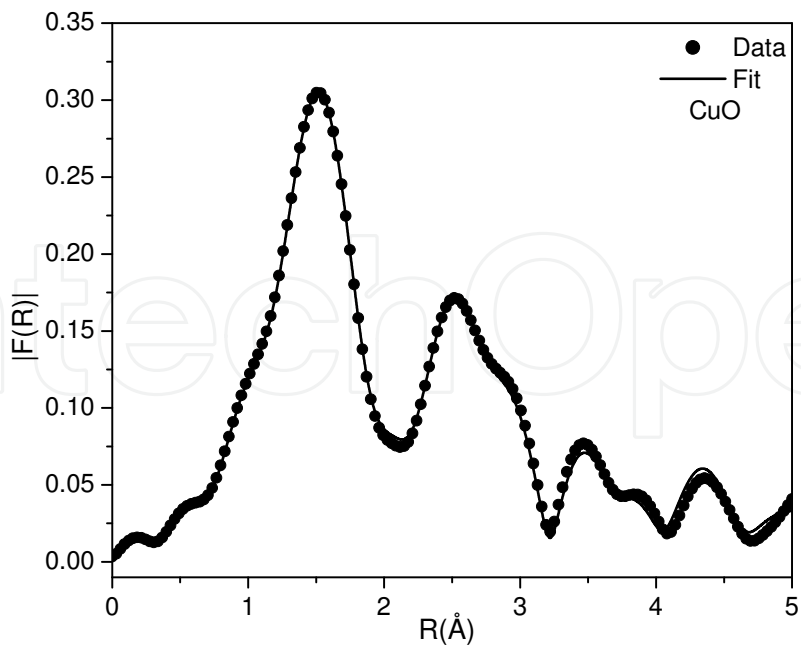Fig. 10. X–ray absorption spectra of annealed Cu_2O thin at 150, 300, 400 and 500°C in air

Fig. 11. Theoretical |F(R)| of the EXAFS spectrum at Cu K-edge obtained by the least squares refinement compared to the observed |F(R)| for the Cu₂O thin film annealed at 150°C

Fig. 12. Theoretical |F(R)| of the EXAFS spectrum at Cu K-edge obtained by the least squares refinement compared to the observed |F(R)| for the Cu₂O thin film annealed at 500°C

4. Fabrication and characterisation of CuO/Cu₂O heterojunction

In order to fabricate CuO/Cu$_2$O thin film hetorojunction, thin films of n-type Cu$_2$O are potentiostatically electrodeposited on a Ti substrate in an acetate bath and are annealed at 500 °C for 30 min. in air for the growth of p-type CuO thin films. Thin films of Cu$_2$O are potentiostatically electrodeposited on Ti/CuO electrodes at different deposition potentials Vs SCE while maintaining the same electrolytic conditions, which used to deposit Cu$_2$O on the Ti substrate. Deposition period is varied form 240 min to 120 min in order to obtain sufficient thickness of the films. Film thickness was calculated by monitoring the total charge passed during the film deposition and it was ~1 μm.

Bulk structures of the electrodeposited films on Ti/CuO were studied by the XRD patterns. Fig. 13 shows the XRD patterns of the films deposited on Ti/CuO electrodes at the deposition potentials of -250, -400, -550 and -700 mV Vs SCE. XRD patterns evidence the formation of Cu$_2$O for all deposition potentials on Ti/CuO electrodes while Cu deposition starts in addition to the Cu$_2$O when the film deposited at -700 mV Vs SCE. Single phase Cu$_2$O are possible at the deposition potentials less than -700 mV Vs SCE. XRD patterns further show that peak intensities corresponding atomic reflection of Cu$_2$O increase with deposition potential. It indicates that amount of Cu$_2$O deposit is increased by increasing deposition potential. This is further studied by using SEM.
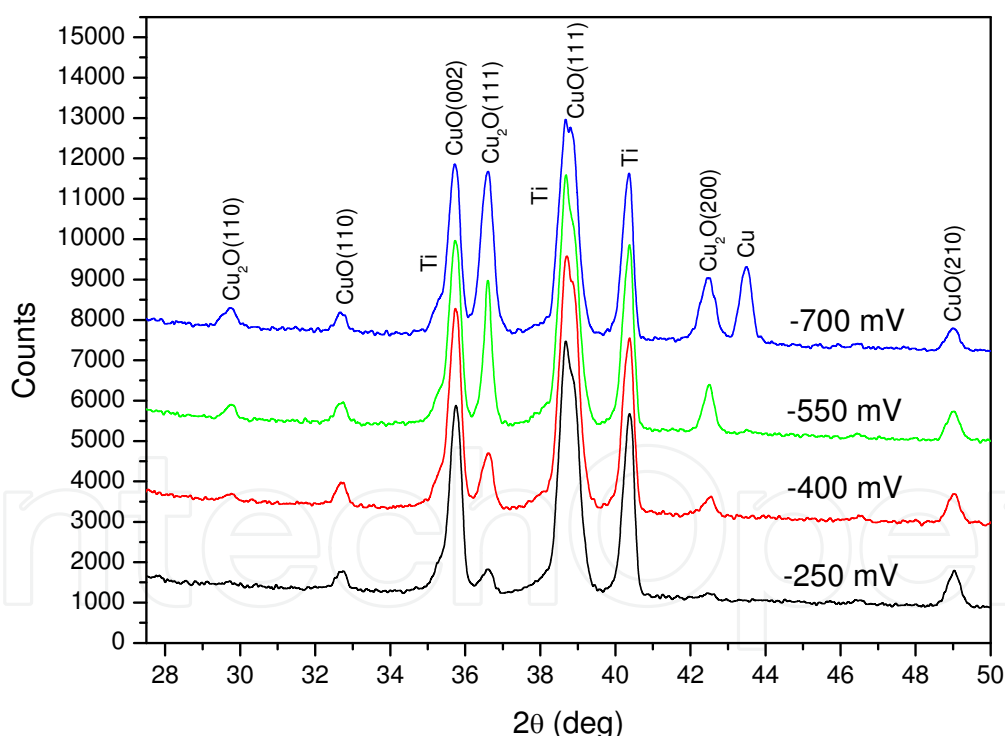

Fig. 13. XRD pattern of thin films electrodeposited on Ti/CuO electrode at the potentials -250, -400, -550 and -700 mV Vs SCE

The surface morphology of the films prepared on the Ti/CuO electrode at the different deposition potentials was studied using the SEMs in order to identify the Cu$_2$O thin film deposition conditions on Ti/CuO electrode. Figs. 14(a) to (c) show the SEMs of Cu$_2$O films deposited on the Ti/CuO at -250 to -550 mV Vs SCE. Fig. 14(a) shows the cubic shape Cu$_2$O

grains on the CuO film and Figs. 14(a) to (c) show that the amount of Cu_2O increases with increasing the deposition potential. The SEMs reveal that the well covered Cu_2O layer can be deposited on Ti/CuO electrode under the potentiostatical condition of -550 mV Vs SCE and above. Grain size of the Cu_2O deposited on Ti substrate is in the range of ~ 1-2 μm as shown in Fig. 14(a) while it is lower to 1 μm when Cu_2O deposited on CuO at the deposition potential of -550 mV Vs SCE. The SEM with low magnification of Cu_2O deposited at -700 mV Vs SCE clearly shows the existence of Cu on the surface of Cu_2O as shown in the XRD pattern of the film deposited at -700 mV Vs SCE.
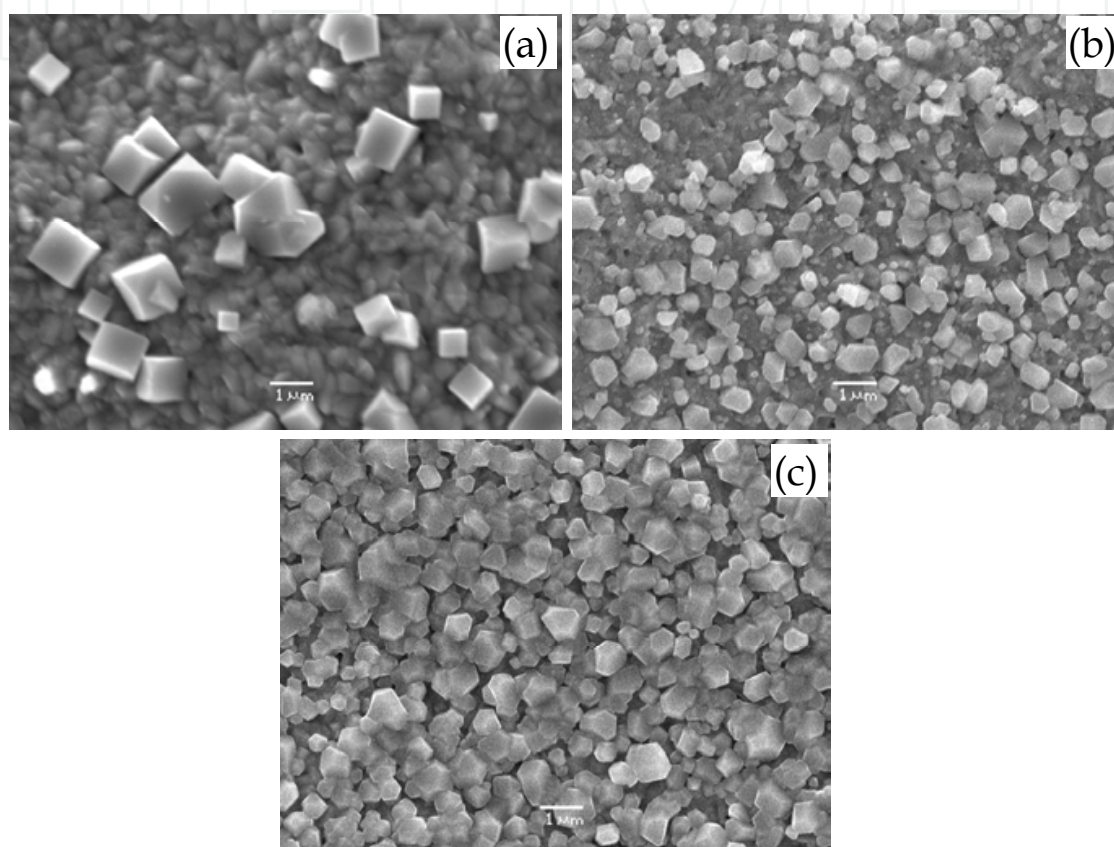
Fig. 14. Scanning electron micrograph of Cu_2O thin films electrodeposited on Ti/CuO electrode at (a) -250 mV, (b) -400 mV and (c) -550 mV Vs SCE

XRD and SEM reveal that well-covered single phase polycrystalline Cu_2O thin film on the Ti/CuO electrode can be possible at the deposition potential of −550 mV Vs SCE in an acetate bath. Structural matching of two semiconductors is very essential for fabricating a heterojunction. In general, the cubic-like Cu_2O grains and the monoclinic-like CuO grains are not match with each other to make the CuO/Cu₂O heterojunction. However, the electrodeposition technique produces the good matching of the Cu_2O grains to the monoclinic-like CuO grains. The shape of the grains can be easily changed when the electrodeposition technique is used to grow a semiconductor. The electrodeposition is a very good tool to fabricate the heterojunctions as it does not depend on the grain shape of the material. Further, the SEMs of the Cu_2O/CuO heterojunction suggested that the Cu_2O polycrystalline grains are grown from the surfaces of the CuO polycrystalline grains and make the good contacts between two thin film layers. For the completion of the device, very

thin (few angstroms) Au grid consists of 1×8 mm^2 rectangular areas are deposited on Cu$_2$O using a vacuum sputtering technique. The electrical contacts to the Cu$_2$O surface (front contacts) is made using mechanically pressed transparent ITO plate to the Au grid, where the Ti substrate serves as back electrical contact to the CuO surface. The Ti/CuO/Cu$_2$O/Au heterojunction gave the open circuit voltage (V$_{oc}$) of 210 mV, short circuit current (J$_{sc}$) of 310 µA cm^2, fill factor (FF) of 0.26 and efficiency (η) of 0.02% under the white light illumination of 90 mWcm^{-2}. At the initial stage of fabrication the junction, the shape of the I–V characteristic as shown in Fig. 15 and values of V$_{oc}$ and J$_{sc}$ are encouraging despite the low photoactive performance of the heterojunction.
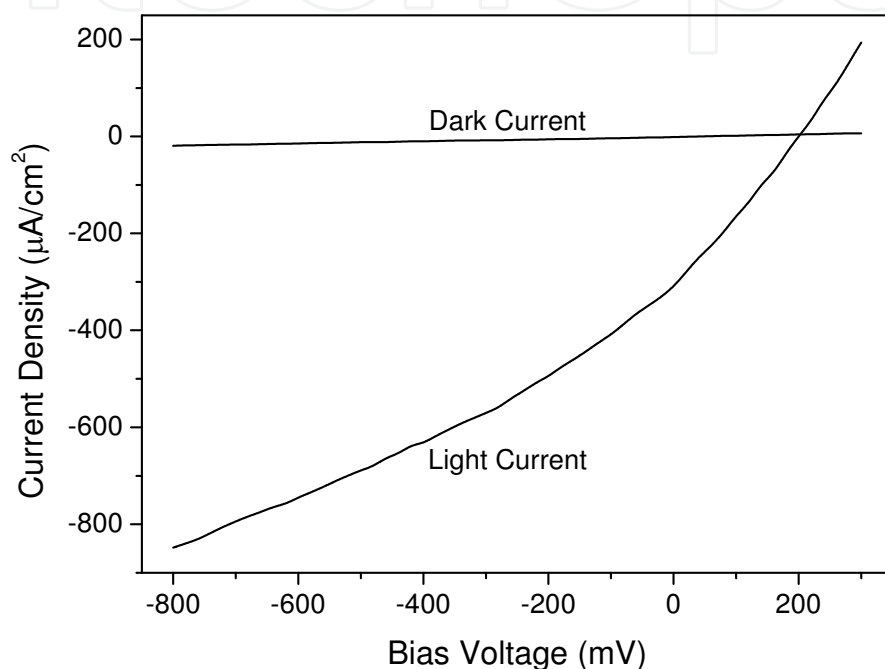
Fig. 15. Dark and light current-voltage characteristics of Ti/CuO/Cu$_2$O/Au heterojunction under the white light illumination of 90 mW/cm^2

For the better performance, very thin Cu$_2$O films should be used due to the high resistance of electrodeposited Cu$_2$O and should be find out better ohmic contact to the Cu$_2$O. Best omic contact to the n-type Cu$_2$O may be Al but not the Au. Au is very good omic contact to p-type Cu$_2$O. n-type electrodeposted Cu$_2$O has high resistivity is due to low doping density. Growth of the n-type Cu$_2$O with suitable dopent hasn't been achieved in the litterateur and it will be very important in developing Cu$_2$O based solar cells.

CuO/Cu$_2$O heterojunction was further investigated by means of X-ray diffractions and X-ray absorption spectra (XAS) at the Cu-K edge with grazing angle measurements. Layer by layer structural information of the CuO/Cu$_2$O heterojunction can be studied with grazing angle measurements. Fig. 16 shows the grazing angle (φ) dependency of the X-ray diffraction patterns of the CuO/Cu$_2$O heterojunction. The Ti peak of highest intensity at $2\theta = 40\cdot23$ degree is indexed by (0,1,1) and (1,1,1) reflections of hexagonal structure and are not observed below $\varphi \sim 2\cdot0$ degree. On the other hand, the reflections of Cu$_2$O and CuO structures are observed in all the grazing angles, though the reflections of Cu$_2$O structure shows the different grazing angle dependence to those of the CuO ones. Fig. 17 shows grazing angle dependency of (1,1,1) reflection of Cu$_2$O, (1,1,-1) reflection of CuO, (1,1,1) reflection of Ti, and intensity ratio of

Cu$_2$O(1,1,1) and CuO(1,1,-1) reflections. The results suggest that Cu$_2$O grain layer can only be observed below φ = 0·1 degree. With increasing the grazing angle, CuO grain layer can be observed gradually, as Ti-reflections. The bulk structural information of Cu$_2$O layer can be obtain for the grazing angles around 2.5 degree since it produces highest intensity of (1,1,1) reflection of Cu$_2$O. It reveals that it is possible to obtain optimum structural information within the Cu$_2$O/CuO junction region in addition to the Cu$_2$O, CuO, and Ti for the grazing angles slightly grater than 2.5 degree. Further it is found that the intensity ratio of the (1,1,1) reflection and (1,1,-1) reflection is approximately constant above φ = 5·0 degree, in contrast to the intensity of the Ti-reflection. It shows that the bulk structural information of bi-layer (Cu$_2$O and CuO) can be studied at the grazing angle 5 degree or greater
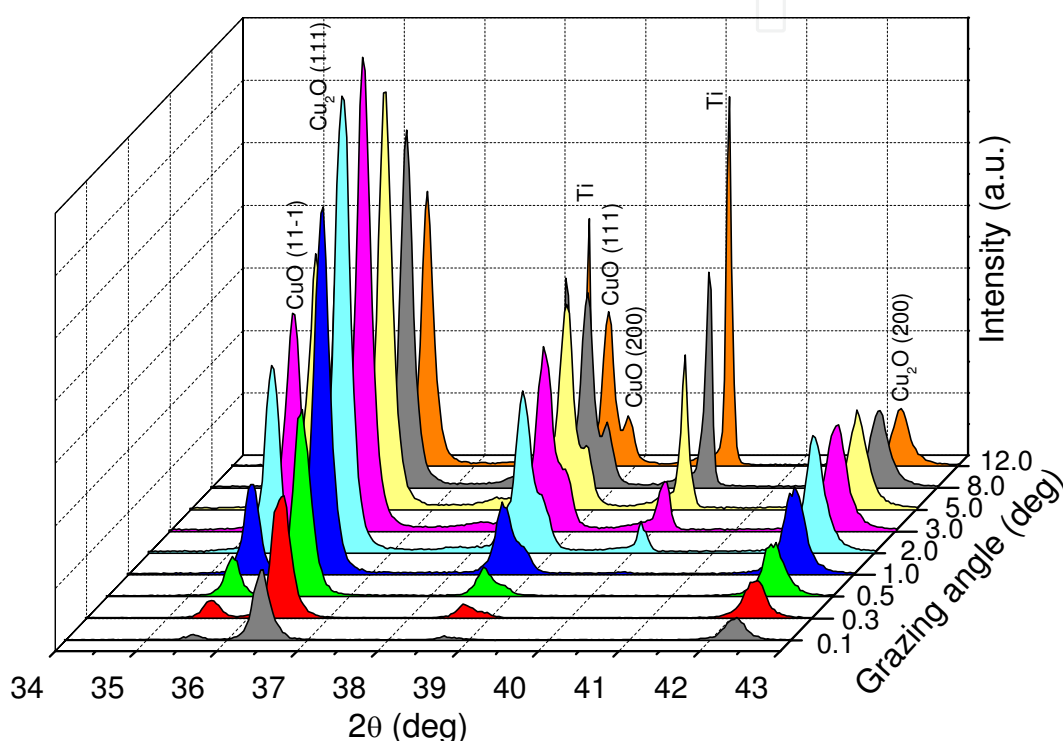

Fig. 16. Grazing angle dependency of the X-ray diffraction patterns for the electrodeposited Ti/CuO/Cu$_2$O heterojunction

The structural deformation localized around Cu ions of the CuO/Cu$_2$O heterojunction can be investigated from EXAFS. Fig. 18 shows the expanded partial XAS at Cu-K edge of Ti/CuO/Cu$_2$O heterojunction at φ = 0·3 to 10·0 deg. The electrodeposited CuO/Cu$_2$O thin film heterojunction include Cu ions sited at different structures of Cu$_2$O and CuO. The spectra result from a convoluted XAS induced by interference between the X-ray photoelectron waves emitted by X-ray absorbing Cu ions and the backscattering waves of its surrounding ions for both structures. The grazing angle dependency of the XAS suggests that the incident X-ray beam penetrate the thin films of Cu$_2$O and CuO grains by the different path distance. It can be considered that the XAS measurements obtained at low grazing angles (0.3 and 0.5 deg) should be mainly the XAS of Cu$_2$O thin film, which is the front layer of the heterojunction. Therefore, the XAS at φ = 0.5 and 3.0 deg are compared with the observed XAS of the electrodeposited thin films of Cu$_2$O and CuO. Fig. 19 shows the comparsion of the expanded partial XAS at grazing angles of 0.5 and 3.0 deg and of the
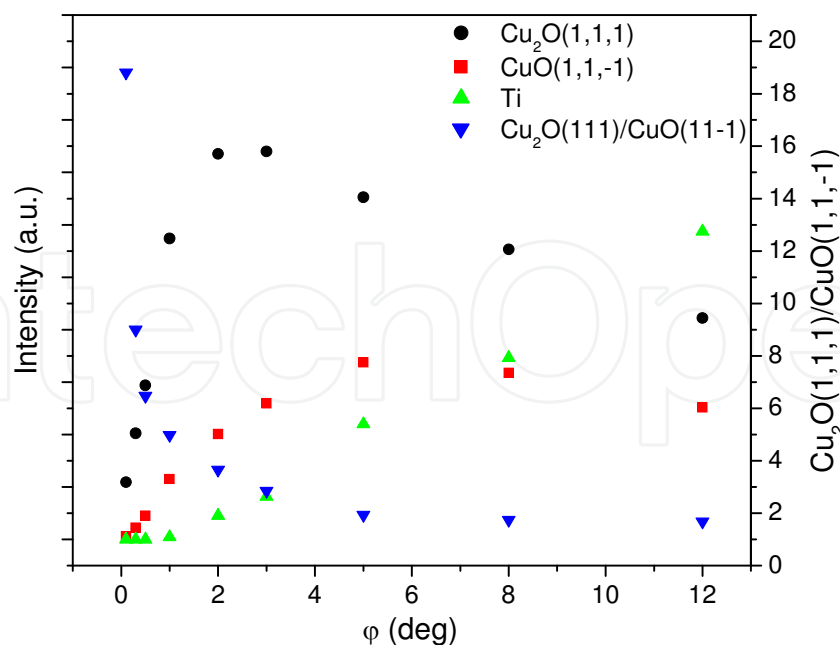
Fig. 17. Grazing angle dependency of the (1,1,1) reflection of the Cu₂O, (1,1,-1) reflection of the CuO structure, the (1,1,1) reflection of Ti and intensity ratio of Cu₂O (1,1,1) and CuO (1,1,-1) reflections

electrodeposited Cu_2O and CuO thin films, in addition to the calculated one of ($0 \cdot 5Cu_2O$ + $0 \cdot 5CuO$). However, XAS (local structure around Cu ions) at low grazing angles are not similar with Cu_2O. It shows that the XAS obtained at even low grazing angles are the convoluted spectra induced by the Cu_2O and CuO structures. The convolution effect of the XAS can be studied by fitting the observed XAS at $\varphi = 0.5$ deg from a simple mathematical convolution of Cu_2O-XAS and CuO-XAS. Fig. 19 shows that the observed XAS at $\varphi = 0.5$ deg is very similar to the calculated one of $0.5(Cu_2O$-XAS) + $0.5(CuO$-XAS). However, XAS at low grazing angles can be analyzed by a simple mathematical convolution of Cu_2O and CuO structures but not for the grazing angles higher than 0.5 deg. This reveals that the complex XAS results from the convoluted spectra induced from unknown structure in addition to the Cu_2O and CuO structures. The XAS modulation due to the unknown structure depends on the grazing angles, and the maximum XAS modulation appears at the grazing angle of 3.0 deg. This suggests that the junction region has very complex structure.

XAS of CuO/Cu_2O hetrojunction with different grazing angles can be further compared by studying corresponding Fourier transformations of the oscillating EXAFS spectra. Fig. 20 shows the observed $|F(R)|$ for the bi-layer thin film of $Ti/CuO/Cu_2O$ heterojunction at $\varphi = 0 \cdot 5$ and $3 \cdot 0$ degrees and for the electrodeposited Cu_2O and CuO thin films with calculated one of ($0 \cdot 5Cu_2O$ + $0 \cdot 5CuO$). It is further confirmed that the $|F(R)|$ obtained at $\varphi = 0 \cdot 5$ and $3 \cdot 0$ degrees are not similar with that of Cu_2O structure and CuO one, but more complex. Comparison between the $|F(R)|$ of the bi-layer thin film obtained at $\varphi = 0 \cdot 5$ degree and the calculated one of ($0 \cdot 5Cu_2O$ + $0 \cdot 5CuO$) suggests that the $|F(R)|$ of the bi-layer thin film is also convoluted by those of the Cu_2O and CuO structures. As in Fig. 20 peak amplitudes are very small for the $|F(R)|$ at $\varphi = 3.0$ deg compared to the others. It implies that structure in the junction region is diluted one (the surrounding ions around the Cu absorbing ion do not well arranged). Results reveal that the formation of amorphous structure in the interface of CuO/Cu_2O heterojunction. It can be expected that amorphous
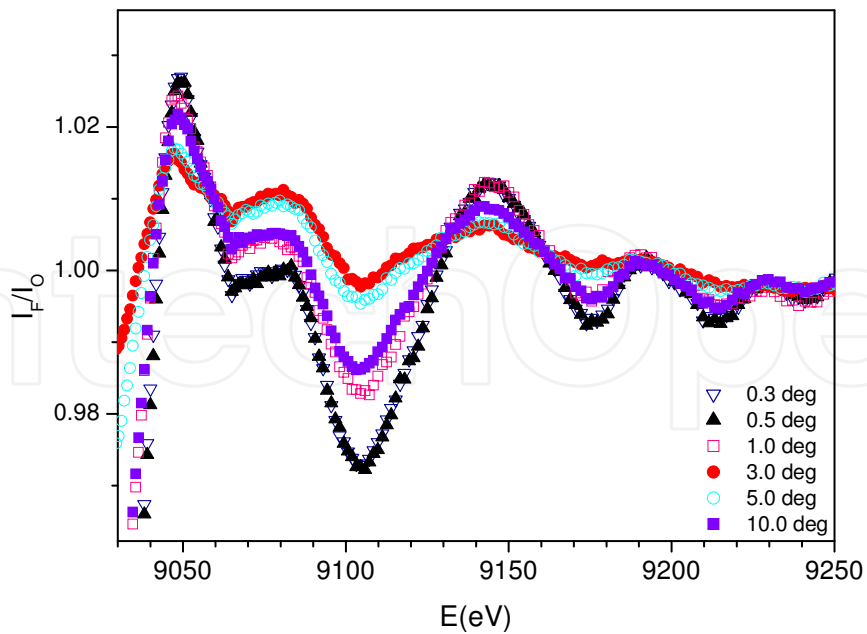
Fig. 18. Oscillating amplitudes I_F/I_o of the X–ray absorption spectra of the Ti/CuO/Cu₂O heterojunction at φ = 0·3 to 10·0 degrees
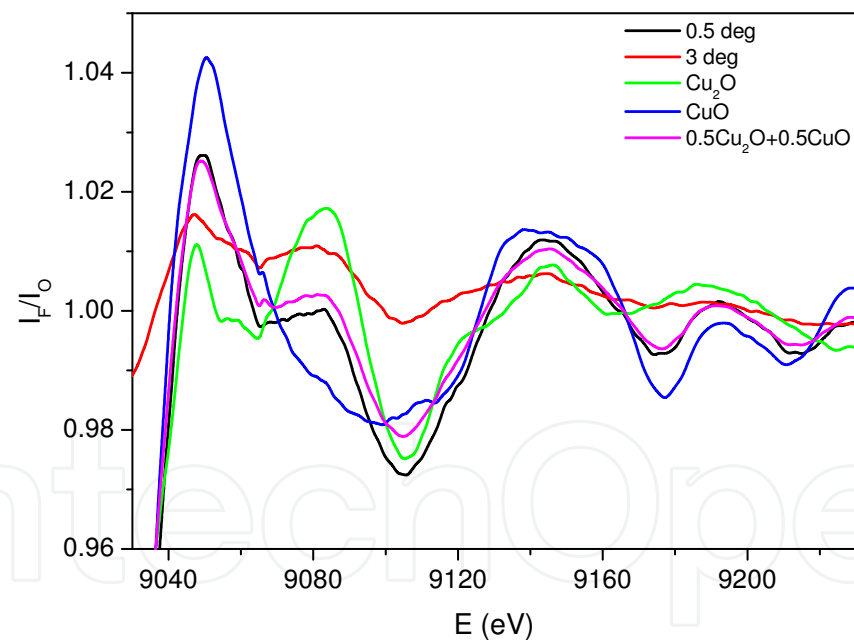

Fig. 19. Oscillating amplitudes I_F/I_o of the X–ray absorption spectra of the Ti/CuO/Cu₂O heterojunction at grazing angles of 0.5 and 3.0 degrees and of the electrodeposited Cu₂O and CuO thin films, in addition to the calculated one of (0·5Cu₂O + 0·5CuO)

structure formed in the middle of the CuO/Cu₂O heterojunction attributes better lattice matching between CuO and Cu₂O interface. Further, it can be considered that formation of the smooth energy band lineup at the interface of CuO/Cu₂O heterojunction without spikes at the conduction and valance bands (ΔE_c and ΔE_v). Band lineup between two semiconductors is a crucial parameter leading to better photoactive properties.
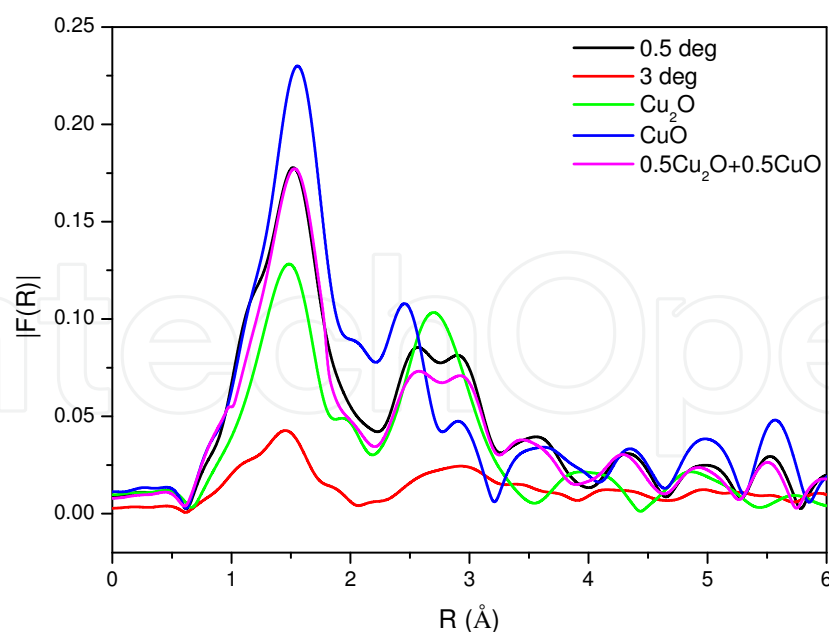
Fig. 20. Amplitudes |F(R)| obtained from the Fourier transformation of the EXAFS spectra of the Ti/CuO/Cu₂O heterojunction at φ = 0·5 and 3·0 degrees and of the electrodeposited Cu₂O and CuO thin films and the calculated one of (0·5Cu₂O + 0·5CuO)

5. Conclusion

Single phase polycrystalline Cu₂O thin films on Ti substrate can be electrodeposited using an acetate bath in a potential range of 0 to -300 mV Vs SCE. Thin films are well adherent to the Ti substrate and uniform having grain size of ~1-2 μm. Cu₂O deposited in an acetate bath at the pH of 6.6 produces n-type photoconductivity in a PV applications. The n-type photoconductivity of the as-grown Cu₂O thin film can be converted to p-type by annealing the films at 300 ᵒC in air. Therefore, it is reasonable to believe that the origin of the n-type Cu₂O is the oxygen ion vacancies created in the crystal lattice, and the conductivity-type conversion is due to the increment of the oxygen content in the lattice with annealing in air. Single phase polycrystalline CuO thin films can be prepared by annealing the electrodeposited Cu₂O at 500 ᵒC for 30 min in air. Films produce p-type photoresponse in a PEC. Well covered n-type Cu₂O thin film can be electrodeposied on Ti/CuO electrode at -550 mV Vs the SCE in an acetate bath. Films consist of microcrystallites of about 1 μm and are well adherent to the CuO. By depositing a suitable mettle grid on the Cu₂O thin film, p-CuO/n-Cu₂O heterojunction solar cell can be fabricated. The Ti/CuO/Cu₂O/Au heterojunction solar cell results in V_{oc} of 210 mV and J_{sc} of 310 μA. This initial stage performance can be enhanced by depositing very thin Cu₂O films leading to minimize the resistance of the Cu₂O and choosing better ohmic contact to the Cu₂O. Best ohmic contact to the n-type Cu₂O may be Al but not the Au. X-ray diffractions and the X-ray absorption spectra, using the synchrotron radiation, reveal that Cu₂O and CuO are high quality semiconducting thin films (free of amorphous phases) but amorphous structure is formed between CuO and Cu₂O while Cu₂O deposition on CuO.

6. Acknowledgment

## 7. References

Akimoto, K., Ishizuka, S., Yanagita, M., Nawa, Y., Goutam K. P. & Sakurai, T. (2006). Thin film deposition of Cu₂O and application for solar cells. *Sol. Energy*, Vol. 80, 715-722

Anandan, S., Wen, X. & Yang, S. (2005). Room temperature growth of CuO nanorod arrays on copper and their application as a cathode in dye-sensitized solar cells. *Mater. Chem. Phys.*, Vol. 93, 35-40

Aveline, A. & Bonilla, I. R. (1981). Spectrally selective surfaces of cuprous oxide (Cu₂O). *Sol. Energy Mater.*, Vol. 5, 2, 211-220

Fortin, E. & Masson, D. (1981). Photovoltaci effects in Cu₂O-Cu cells growing by anodic oxidation. *Solid-St. Electron.*, Vol. 25, 4, 281-283

Garuthara, R. & Siripala, W. (2006). Photoluminescence characterization of polycrystalline n-type Cu₂O films. *J. Luminescence*, Vol. 121, 173-178

Ghijsen, J., Tjeng, L.H., Elp, J. V., H. Eskes, Westerink, J., & Sawatzky, G.A. (1988). Electronic structure of Cu₂O and CuO. *Phys. Rev.*, Vol. 38, 11322-11330

Guy, A. C. (1972). *Introduction to Material Science (International Student Edition)*, McGraw-Hill, Tokyo

Hames,Y. & San, S. E. (2004).CdO/Cu₂O solar cells by chemica deposition. *Sol. Energy*, Vol. 77, 291-294

Harukawa, N., Murakami, S., Tamon, S., Ijuin, S., Ohmori, A., Abe, K. & Shigenari, T. (2000). Temperature dependence of luminescence lifetime in Cu₂O. *J. Luminescence*, Vol. 87-89, 1231-1233

Herion, J., Niekisch E. A. & Scharl, G. (1980). Investigation of metal oxide/cuprous oxide heterojunction solar cell. *Sol. Energy Mater.*, Vol. 4, 101-112

Ivill, M., Overberg, M. E., Abernathy, C. R., Norton, D. P., Hebard, A. F., Theoropoulou, N. & Budai, J. D. (2003). Properties of Mn-doped Cu₂O semiconducting thin films grown by pulsed-laser deposition. *Solid-St. Electronics*, Vol. 47, 2215-2220

Kaufman, R. G. & Hawkins, R. T. (1984). Defect luminescence of thin films of Cu₂O on copper. *J. Electrochem. Soc.*, Vol. 131, 385-388

Mahalingam, T., Chitra, J. S. P., Chu, J. P. & Sebastian, P. J. (2004). Preparation and microstructural studies of electrodeposited Cu₂O thin films. *Mater. Lett.*, Vol. 58, 1802-1807

Mahalingam, T., Chitra, J. S. P., Rajendran, S. & Sebastian, P. J. (2002). Potentiostatic deposition and characterisation of Cu₂O thin films. *Semicond. Sci. Technol.*, Vol. 17, 565- 570

Mahalingam, T., Chitra, J. S. P., Rajendran, S., Jayachandran, M. & Chockalingam, M. J. (2000). Galvanostatic deposition and characterization of cuprous oxide thin films. *J. Crys. Growth*, Vol. 216, 304-310

Maruyama, T. (1998). Copper oxide thin films prepared by chemical vapor deposition from copper dipivaloylmethanate. *Sol. Energy Mater. Sol. Cells*, Vol. 56, 85-92

Musa, A. O., Akomolafe, T. & Carter, M. J. (1998). Production of cuprous oxide, a solar cell material, by thermal oxidation and a study of its physical and electrical properties. *Sol. Energy Mater. Sol. Cells*, Vol. 51, 305-316

Ogwa, A. A., Bouquerel, E., Ademosu, O., Moh, S., Crossan, E. & Placido, F. (2005). An investigation of the surface energy and optical transmittance of copper oxide thin films prepared by reactive magnetron sputtering. *Acta Materialia*, Vol. 53, 5151-5159

Olsen, L. C., Addis, F. W. & Miller, W. (1981-1983). Experimental and theoretical studies of Cu_2O solar cells. *Sol. Cells*, Vol. 7, 247-279

Papadimitriou, L., Economou N. A. & Trivich, D. (1981). Heterojunction solar cells on cuprous oxide. *Sol. Cells*, Vol. 3, 73-80

Paul, G. K., Nawa, Y., Sato, H., Sakurai, T. & Akimoto, K. (2006). Defects in Cu_2O studied by deep level transient spectroscopy. *Appl. Phys. Lette.*, Vol. 88, 141900

Pollack, G. P. & Trivich, D. (1975). Photoelectric properties of cuprous oxide. *J. Appl. Phys.*, Vol. 46, 163-173

Rai, B. P. (1988). Cu_2O solar cells: a review. *Sol. Cells*, Vol. 25, 265-272

Rakhshani, A.E. (1986). Preparation, charaterestics and photovoltaic proporties of cuprus oxide – a review. *Soild State Electronics*, Vol. 29, No. 1, 7-17

Rakhshani, A. E. & Varghese, J. (1988). Potentiostatatic electrodeposition of cuprous oxide. *Thin Solid Films*, Vol. 157, 87-95

Rakhshani, A. E. & Varghese, J. (1987). Galvanostatic deposition of thin films of cuprous oxide. *Sol. Energy Mater.*, Vol. 15, 237-248

Roos, A., Chibuye, T. & Karlsson, B. (1983). Proporties of oxide copper sufaces for solar cell applications II. *Sol. Energy Mater.*, Vol. 7, 453 467-480

Santra, K., Chitra, C. K., Mukherjee, M. K. & Ghosh, B. (1992). Copper oxide thin films grown by plasma evaporation method. *Thin Solid Films*, Vol. 213, 226-229

Sears, W. M., Fortin, E. & Webb, J. B. (1983). Indium tin oxide/Cu_2O photovoltaic cells. *Thin Solid Film*, Vol. 103, 303–309

Sears, W. M. & Fortin, E. (1984). Preparation and properties of Cu_2O/Cu photovoltaic cells. *Sol. Energy Mater.*, Vol. 10, 93-103

Siripala, W., Perera, L. D. R. D., De Silva, K. T. L., Jayanetti, J. K. D. S., & Dharmadasa, I. M. (1996). Study of annealing effects of cuprous oxide grown by electrodeposition technique. *Sol. Energy Mater. Sol. Cells*, Vol. 44, 251-260

Siripala, W. & Jayakody, J. R. P. (1986). Observation of n-type photoconductivity in electrodeposited copper oxide film electrodes in a photoelectrochemical cell. *Sol. Energy Mater.*, Vol. 14, 23-27

Stareck, J. E. (1937). US Patent #2,081,121

Tanaka, H., Shimakawa, T., Miyata, T., Sato H. & Minami, T. (2004). Electrical and optical properties of TCO–Cu_2O heterojunction devices. *Thin Solid Films*, Vol. 469, 80-85

Tang, Y., Chen, Z., Jia, Z., Zhang, L. & Li, J. (2005). Electrodeposition and characterization of nanocrystalline cuprous oxide thin films on TiO_2 films. *Mater. Lett.*, Vol. 59, 434-438

Tiwari, A.N., Pandya, D.K. & Chopra, K.L. (1987). Fabrication and analysis of all-sprayed $CuInS_2$/ZnO solar cells. *Solar Cells*, Vol. 22, 263-173

Wijesundera, R.P., Hidaka, M., Koga, K., Sakai, M., & Siripala,W. (2006). Growth and characterisation of potentiostatically electrodeposited Cu_2O and Cu thin films. *Thin Solid Films*, Vol. 500, 241-246

Wijesundera, R. P., Perera, L. D. R. D., Jayasuriya, K. D., Siripala, W., De Silva, K. T. L., Samantilleka A. P. & Darmadasa, I. M. (2000). Sulphidation of electrodeposited cuprous oxide thin films for photovoltaic applications. *Sol. Energy Mater. Sol. Cells,* Vol. 61, 277-286

Wijesundera, R. P. (2010). Fabrication of the CuO/Cu_2O heterojunction using an electrodeposition technique for solar cell applications. *Semicond. Sci. Technol.*, Vol. 25, 1-5

Wijesundera, R.P., Hidaka, M., Koga, K., Sakai, M., Siripala, W., Choi, J.Y. & Sung, N. E. (2007). Effects of annealing on the properties and structure of electrodeposited semiconducting Cu-O thin films, *Physica Status of Solidi (b)*, Vol. **244,** 4629-4642
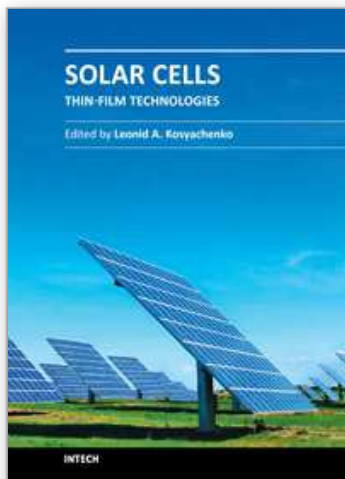
Solar Cells - Thin-Film Technologies

Edited by Prof. Leonid A. Kosyachenko

The first book of this four-volume edition is dedicated to one of the most promising areas of photovoltaics, which has already reached a large-scale production of the second-generation thin-film solar modules and has resulted in building the powerful solar plants in several countries around the world. Thin-film technologies using direct-gap semiconductors such as CIGS and CdTe offer the lowest manufacturing costs and are becoming more prevalent in the industry allowing to improve manufacturability of the production at significantly larger scales than for wafer or ribbon Si modules. It is only a matter of time before thin films like CIGS and CdTe will replace wafer-based silicon solar cells as the dominant photovoltaic technology. Photoelectric efficiency of thin-film solar modules is still far from the theoretical limit. The scientific and technological problems of increasing this key parameter of the solar cell are discussed in several chapters of this volume.

How to reference

In order to correctly reference this scholarly work, feel free to copy and paste the following:

INTECH

open science | open minds